Atmos. Chem. Phys. Discuss.,
https://doi.org/10.5194/acp-2017-644-AC2, 2017

Interactive comment on "First tomographic observations of gravity waves by the infrared limb imager GLORIA" *by* Isabell Krisch et al.

Isabell Krisch et al.

i.krisch@fz-juelich.de

Received and published: 26 October 2017

Dear Referee #2,

Thank you very much for these very helpful comments!

To increase the visualization of the paper, Figures 2 and 3 will be updated according to remarks #25 and #26. According to comment #33, the physical meaning of the total momentum, which is a measure for the drag, a GW event can exert on the atmosphere, will be better explained. This number is especially important as it can be compared to the GW drag of GCMs and cannot be provided by 1D wind observations. Comment

#34 has been mentioned in a similar way by all referees. We will include more details on how the occurrence probabilities were determined. A similar distribution derived from GLORIA measurements (comment #39), cannot be provided, as tomographic measurement patterns are event based only and, thus, not suitable for a statistical analysis. We very much appreciate remark #44 and will extend the discussion on the different results of 1D and 4D ray-tracing, respectively. Further we will include a paragraph on how the results of our paper can advance GW parameterizations.

In addition, we will address all other minor comments in the paper. A detailed list of all changes can be found below.

Again, thank you very much for helping us to present the theoretical background accurately and for improving the discussion and interpretation of results.

Sincerely, Isabell Krisch

Reviewer comment: Page 1, Line 2-3, the term 'global atmospheric circulation models'. Even there are more than one options, mostly GCM refers to 'general circulation model'.
Authors response: All occurrences of 'global atmospheric circulation models' will be replaced by general circulation model.

Reviewer comment: Page 1, Line 5, measured - observed/revealed.
Authors response: This will be changed in the manuscript.

Reviewer comment: Page 1, Line 12-13, the last sentence should be reworded.
Authors response: The last sentence of the abstract will be reworded.
Text changes: Forward ray-tracing reveals that the waves propagate laterally more than 2000 km away from their source region. A comparison of a 3D ray-tracing version to solely column based propagation showed that lateral propagation can help the waves to avoid critical layers and propagate to higher altitudes. Thus, the implementation of oblique gravity wave propagation into general circulation models may improve their predictive skills.

Reviewer comment: Page 1, Line 17, I do not see a good logic relation when using 'Thereby'.
Authors response: The relation between the two sentences will be clarified.
Text changes: The exerted drag induces the meridional circulation in the mesosphere / lower thermosphere (MLT) and finally leads to the cold summer mesopause and the warm winter stratopause.

Reviewer comment: Page 1, Line 20, add abbreviation QBO for quasi-biennial oscillation.
Authors response: The abbreviation will be added.

Reviewer comment: Page 2, Line 14, there are more published papers about the gravity wave parameterization schemes such as Alexander and Dunkerton 1999, Beres et al. 2004 and 2005, Richter et al. 2010. Page 2, Line 15, besides the source distribution, the launched wave propagation direction is another simplification.
Authors response: A more detailed list of references on GW parameterization schemes will be included. The simplifications in the source distributions have been mentioned.

Reviewer comment: Page 2, Line 24, polarization - polarisation, analyzed - analysed, you may skip this since they are just differences between American and Bristish English.
Authors response: This will be addressed in the revised manuscript.

Reviewer comment: Page 2, Line 25, there are several published papers using multiple instruments (colocated or network) to study the 3D strucuture of gravity waves such as Lu et al. 2016 (two lidar and imager), Cao et al. 2016 (lidar and imager), Bossert et al. 2015 (lidar and imager).
Authors response: The mentioned further examples of 3D measurements in the mesosphere have been mentioned in the manuscript. However, these measurements have the same restriction as the MAARSY measurements, that they are far away from the sources and limited to few ground based stations.
Text changes: In the mesosphere, a full wave characterization of short scale GWs has been achieved with the Middle Atmosphere Alomar Radar System (MAARSY; Stober et al., 2013). For medium scale GWs in the mesosphere, a full characterization has been derived by combining lidar and airglow imager measurements (Bossert et al., 2015; Lu et al., 2015; Cao et al., 2016). However, all these observations are limited to a few ground based stations. Further, it is difficult to link observations at altitudes as high as the mesopause region to specific GW sources, which are usually located at much lower altitudes in the troposphere and lower stratosphere. So far no measurement technique existed to measure the 3D structure of mesoscale GWs in the lower stratosphere.

Reviewer comment: Page 3, Line 5, remove 'measurement'
Authors response: This word will be removed.

Reviewer comment: Page 3, Line 7, the title of this section could better be 'Data and

Methodolody'. Page 7, Section 3 title 'Analysis'-'Results'.
Authors response: Both section titles will be changed.

Reviewer comment: Page 3, Line 18, I suppose less pixels are used thus the readout time is reduced.
Authors response: This will be addressed in the text.

Reviewer comment: Page 3, Line 23, what is the aircraft flight altitude? what is the altitude range the measurements are taken?
Authors response: These points will be included in the manuscript.
Text changes: The aircraft flight altitude during this time was between 12.5 km and 13.5 km. Towards low altitudes, the GLORIA measurements were limited by clouds reaching up as far as 9 km to 10.5 km.

Reviewer comment: Page 4, table 1 caption, the second sentence: The last column indicates the retrieved quantity for each spectral range.
Authors response: This will be changed in the text.

Reviewer comment: Page 4, Line 12, this part - which part? the altitude range?
Authors response: This will be changed in the text.

Reviewer comment: Page 5, Line 7, what is the temporal resolution, such as the integration time or exposure time?
Authors response: A sentence on the temporal resolution will be added to Sec. 2.1.
Text changes: The time needed to accomplish the hexagon was about 2 h. During this time 2200 infrared images and corresponding spectra were taken. The presented tomographic retrieval represents a temporal mean over all these measurements.

Reviewer comment: Page 5, Line 9-10, what is the evidence that this is a mountain wave? This is important because this is the prerequisite of fitting. Is it stationary or near stationary during your 2 hour observation window?
Authors response: These waves were predicted by the ECMWF forecast to be stationary above Iceland for more than 6 hours. This will be included in the text.

Reviewer comment: Page 5, Line 12, remove 'as discussed in Sec. 3.2'. It is not proper to refer to something in latter discussions.
Authors response: This will be removed.

Reviewer comment: Page 5, Line 17, 'GW'-'GWs'.
Authors response: This will be changed.

Reviewer comment: Page 5, Line 18-19, what is the relation between S-G filter and the polynomial fitting?
Authors response: The method proposed by (**?**), which is called Savitzky-Golay filter, is based on a so-called running polynomial fitting. A polynomial of order k is fitted to a box of n neighbouring points and the middle point is replaced by the value of the fit. This is done for all data points by shifting the boxes over the data. Thus, Savitzky-Golay filter is a common name for polynomial filter.
Text changes: This was done through applying SG filters to the GLORIA temperature data in all three dimensions. For the SG filtering, 3rd order polynomials were fitted to 25, 60, and 60 neighbouring points in the vertical, zonal, and meridional directions.

Reviewer comment: Page 6, Figure 2, I feel Fig. 2 could be improved for better visulization. Add x - y - z coordinate to show the scale of wave structures. The

colorbar for positive and negative temperature perturbation should be properly chosen (redwhite-blue) to clearly demonstrate the wave pattern. Figure 3 of Wright et al. 2017 is a good example.
Authors response: Fig. 2 will be changed according to the remarks.

Reviewer comment: Page 6, Line 1, 'direction'-'directions', 'taken'-'treated'. Page 6, Line 2, 'can be seen' - 'is demonstrated'.
Authors response: This will be changed.

Reviewer comment: Page 7, Figure 3, the x-coordinate of bottom sub-figures could be just the distance, which is more straightforward to compare the scales of GWs.
Authors response: Fig. 3 D-F now plots distance as x-axis. Furthermore, the colormap of Fig. 3 will be changed to be in agreement with the updated Fig. 2.

Reviewer comment: Page 7, Line 8, and the data plotted in Fig. 2 and Fig. 3, what is the horizontal resolution of the raw temperature measurements? You may clarify these basic information in the text.
Authors response: This information can be found at the end of Sec. 2.1.

Reviewer comment: Page 7, Line 9, '3D direction'- please clarify this direction, is this direction the wave 'propagation direction' or the orientation of the wave front? You assume it is a mountain wave, so the wave is not really 'propagating'. So if it is the orientation of the wave front, is there a relationship between the wave front orientation and the mountain ridge orientation?
Authors response: The 3D direction is the direction of the wave vector $\vec{k} = (k, l, m)$. And the wave vector is oriented perpendicular to the mountain ridge. 2 panels with the horizontal wave vector direction and the orography of Iceland will be added to Fig. 5

(*former Fig. 4*).
Text changes: The fitted parameters are the 3D wave vector $\vec{k} = (k, l, m)$ and the amplitudes (Fig. 5C). Horizontal and vertical wavelengths, and the horizontal wave direction were calculated from the wave vector $\vec{k}$ and shown in Fig. 5A, 5B, and 5E, respectively. Fig. 5F shows the orography of Iceland. The main mountain ridge is oriented in east-west direction. As expected for a mountain wave, the horizontal wave direction (Fig. 5E) is perpendicular to the ridge orientation.

Reviewer comment: Page 7, Line 14, 'the strength of the coupling of a GW with the background', what does this mean? Does it mean the same as the forcing/drag of GW. Page 7, Line 15, at the end add 'when they dissipate.'
Authors response: The misleading expression 'strength of the coupling' will be replaced and the sentence will be reworded.
Text changes: Integrating the GWMF over the horizontal extent of a GW event leads to the total momentum, which determines the maximal drag this GW event can exert on the background flow in coupling and dissipation processes.

Reviewer comment: Page 8, Line 1, since those wave parameters are derived from fitting, are there confidence intervals that can describe the robustness of the fitting, say the uncertainties of those fitted parameters.
Authors response: A discussion of relevant effects for the uncertainty of the fitted parameters and the resulting confidence intervals is given in Appendix A. This will be mentioned here.

Reviewer comment: Page 8, Line 5-6, the total momentum in the order of GN (109N) seems to be a gigantic number, what is the physical meaning of this total momentum? The force the wave exerts on atmosphere? And how do you distinguish these two waves spatially?

Authors response: The total momentum corresponds to the maximal drag a GW event can exert on the background flow in coupling and dissipation processes. The two waves were defined to be north and south of 66.2 N. These points will be clarified in the text.
Text changes: The horizontal distribution of the GWMF clearly highlights two distinct wave packets: one with local GWMF of up to 50 mPa north of 66.2 N and one with local GWMF of up to 100 mPa south of 66.2 N. The GLORIA observations provide the horizontal variations of GWMF at 11.5 km altitude. This allows to integrate over the corresponding area of the two events and calculate the total momentum, a measure for the maximal drag this GW event can exert on the background flow in coupling and dissipation processes. This is a main advantage with respect to 1D wind observations, which can provide peak GWMF values but not the area for which these values are valid.

Reviewer comment: Page 8, Line 7, how do you quantify the GW and calculate MF from ECWMF model? Page 8, Line 8, how do you calculate this 0.14%? Do you mean the largest 0.14% of the all GWs?
Authors response: Similar points were mentioned by all three reviewers. We will include the details on how the occurrence probabilities are determined in the manuscript.
Text changes: To classify this event, a comparison of all GW events in January 2016 has been performed in the 6-hourly operational analyses of ECMWF. First the temperature background was isolated, as described in Sec. 2.1 for the a-priori field, and subtracted from the original field. The remaining temperature residuals were analyzed for GWs using the 3D sinusoidal fit algorithm described above. The GWMFs for all cubes were calculated. The GWMFs from all 124 analyses fields were combined to obtain the probability of GW occurrence (Fig. 6*, former Fig. 5*). Here, all GWMF values were considered independent of the horizontal and vertical wavelengths. Removing wavelengths larger than 2.5 times the cube size in order to filter less significant fits (not shown) induced no major changes in the general shape of the distribution. This indicates that GW events with less certain fits do not bias the probability distribution.

For the GW event over Iceland similar GWMF magnitudes were determined from the ECMWF analyses and from the GLORIA measurements. Thus, a comparison of the measurement results with the occurrence probability determined from the ECMWF analyses seems reasonable. According to Fig. 6 the measured GW event can be classified as a very strong case since the sum of all occurrence probabilities of stronger events is far below 1%.

Reviewer comment: Page 8, Line 14, 'characterize'-locate or identify. Page 8, Line 15, 'advance'-'advantage'.
Authors response: These points will be changed in the manuscript.

Reviewer comment: Page 8, Line 17, in this condition, when ray-tracing is discussed, GW intrinsic parameters rather than MF matter here.
Authors response: This will be changed in the text.

Reviewer comment: Page 9, Figure 5, this is the intermittency of the gravity waves, which is mainly described by this probability distribution. I suppose you can make a similar plot using the MF derived from your observations, which I think makes more sense to quantify the intermittency of the gravity waves retrieved from your observations. If go further, the log-normal distribution can also be fitted in the probability distributions.
Authors response: A similar distribution derived from GLORIA measurements cannot be provided, as tomographic measurement patterns are event based only and, thus, not suitable for a statistical analysis.

Reviewer comment: Page 9, Line 9-10, for each dot of different size, it could be better visualization if you add a white edge for each dot, then they can be still visible

when overlapped with dense trajectories.
Authors response: Fig. 7 will be updated in this respect.

Reviewer comment: Page 9, Line 10-11, 'according to the GWMF at the source location', so here you implicitly assume the GWs do not undergo any dissipation when they propagate from source to measurement locations?
Authors response: This will be addressed in the revised manuscript.
Text changes: These GWMF values are conservative estimates, as the backward ray-tracing cannot account for dissipation processes.

Reviewer comment: Page 9, Line 13-14, what is the point of this 6 hour, in your Figure 6A, you indicate it is a 1-day backward simulation. So is there any conflict between these two? Then, can we understand this time is related to the propagating speed of the wave packet, say how much time it takes to propagate from source to measurement location. If so, a speed (group speed?) could be estimated.
Authors response: We constructed a GROGRAT background atmosphere allowing for backward integration up to one day. However, the rays actually arrived at the mountains already after 6 hours. This will be clarified in the text.
Text changes: As can be seen in Fig. 7C, the ray-traces need between 3 and 6 hours to reach the ground. This is in good agreement with a vertical group velocity of 2 to 3 km/h, which has been calculated from the measurements. Hence, the GWs are probably excited roughly 6 hours before the measurements were taken.

Reviewer comment: Page 10, Line 1-2, the turning of the wave vectors could be explained by the wave refraction.
Authors response: This explanation will be added to the manuscript.
Text changes: Over Eastern Europe, the GWs are refracted by a horizontal wind shear, which changes their horizontal wave vector from southward to westward.

This allows the waves to quickly propagate upward into the westerly wind in the mid stratosphere.

Reviewer comment: Page 11, the ray-tracing simulation (backward and forward) of GW propagation and the comparsion between 1D vs. 4D run are dramatically interesting and important. I expect more discussions about the ray-tracing results, especially on how this study can advance our understanding of the horizontal propagation of GWs and insights into GW parameterization.
Authors response: The authors very much appreciate this comment and will extend the discussion, respectively.
Text changes: Two processes might play a significant role here: First, in the 1D GROGRAT version the GWs are not refracted and the wave vectors do not change its horizontal orientation with altitude. The westerly background winds at higher altitudes do not favor the propagation of GWs with wave vectors perpendicular to the wind direction. Second, in the full GROGRAT run, the GWs propagate horizontally away from the source. Hence, the GWs avoid the critical level positioned above the source location and more GWMF is transported to higher altitudes. Global mountain wave modeling (Xu et al., 2017) suggests that this effect may prevail also on a global basis.

Neither a realistic orientation of the wave vector, nor oblique GW propagation are incorporated in GW parameterizations used in current climate and weather prediction models (McLandress, 1998; Alexander and Dunkerton, 1999; Richter et al., 2010; McLandress et al., 2012; Garcia et al., 2017). However, both processes are context of several studies aiming to improve GW parameterizations (Preusse et al., 2009; Sato et al., 2009; Kalisch et al., 2014; Amemiya and Sato, 2016; Ribstein and Achatz, 2016; Garcia et al., 2017). The present paper provides a strong motivation to finally implement these processes in current climate and weather prediction models. Especially, as this could close gaps of GWMF in regions with sparse sources (McLandress et al., 2012) and reduce the cold-pole bias of climate and weather prediction models in the lower stratosphere (Garcia et al., 2017).

Reviewer comment: Page 14, Line 16, 60.
Authors response: This will be changed in the text.

Reviewer comment: Page 17, please skip the questions regarding the uncertainties of fitted GW parameters.
Authors response: The authors think that the uncertainty discussion is an important part of this paper and therefore prefer to keep these paragraphs.

References

Alexander, M. J. and Dunkerton, T. J.: A Spectral Parameterization of Mean-Flow Forcing due to Breaking Gravity Waves, Journal of the Atmospheric Sciences, 56, 4167–4182, doi:10.1175/1520-0469(1999)056<4167:ASPOMF>2.0.CO;2, 1999.

Amemiya, A. and Sato, K.: A New Gravity Wave Parameterization Including Three-Dimensional Propagation, Journal of the Meteorological Society of Japan. Ser. II, advpub, doi:10.2151/jmsj.2016-013, 2016.

Bossert, K., Fritts, D. C., Pautet, P.-D., Williams, B. P., Taylor, M. J., Kaifler, B., DÃÂűrnbrack, A., Reid, I. M., Murphy, D. J., Spargo, A. J., and MacKinnon, A. D.: Momentum flux estimates accompanying multiscale gravity waves over Mount Cook, New Zealand, on 13 July 2014 during the DEEPWAVE campaign, J. Geophys. Res. Atmos., 120, 9323–9337, doi:10.1002/2015JD023197, http://dx.doi.org/10.1002/2015JD023197, 2015JD023197, 2015.

Cao, B., Heale, C. J., Guo, Y., Liu, A. Z., and Snively, J. B.: Observation and modeling of gravity wave propagation through reflection and critical layers above Andes Lidar Observatory at Cerro PachÃ³n, Chile, J. Geophys. Res. Atmos., 121, 12,737–12,750, doi:10.1002/2016JD025173, http://dx.doi.org/10.1002/2016JD025173, 2016JD025173, 2016.

Garcia, R. R., Smith, A. K., Kinnison, D. E., de la Camara, A., and Murphy, D. J.: Modification

of the Gravity Wave Parameterization in the Whole Atmosphere Community Climate Model: Motivation and Results, J. Atmos. Sci., 74, 275–291, doi:10.1175/JAS-D-16-0104.1, 2017.

Kalisch, S., Preusse, P., Ern, M., Eckermann, S. D., and Riese, M.: Differences in gravity wave drag between realistic oblique and assumed vertical propagation, Journal of Geophysical Research: Atmospheres, 119, 10,081–10,099, doi:10.1002/2014JD021779, 2014.

Lu, X., Chen, C., Huang, W., Smith, J. A., Chu, X., Yuan, T., Pautet, P.-D., Taylor, M. J., Jie, G., and Cullens, C. Y.: A coordinated study of 1 h mesoscale gravity waves propagating from Logan to Boulder with CRRL Na Doppler lidars and temperature mapper, J. Geophys. Res. Atmos., 120, 10,006–10,021, doi:10.1002/2015JD023604, http://dx.doi.org/10.1002/2015JD023604, 2015JD023604, 2015.

McLandress, C.: On the importance of gravity waves in the middle atmosphere and their parameterization in general circulation models, J. Atm. Sol.-Terr. Phys., 60, 1357–1383, doi:10.1016/S1364-6826(98)00061-3, 1998.

McLandress, C., Shepherd, T. G., Polavarapu, S., and Beagley, S. R.: Is Missing Orographic Gravity Wave Drag near 60Â°S the Cause of the Stratospheric Zonal Wind Biases in Chemistry-Climate Models?, J. Atmos. Sci., 69, 802–818, doi:10.1175/JAS-D-11-0159.1, http://dx.doi.org/10.1175/JAS-D-11-0159.1, 2012.

Preusse, P., Eckermann, S. D., Ern, M., Oberheide, J., Picard, R. H., Roble, R. G., Riese, M., Russell III, J. M., and Mlynczak, M. G.: Global ray tracing simulations of the SABER gravity wave climatology, J. Geophys. Res. Atmos., 114, doi:10.1029/2008JD011214, 2009.

Ribstein, B. and Achatz, U.: The interaction between gravity waves and solar tides in a linear tidal model with a 4-D ray-tracing gravity-wave parameterization, Journal of Geophysical Research: Space Physics, 121, 8936–8950, doi:10.1002/2016JA022478, http://dx.doi.org/10.1002/2016JA022478, 2016JA022478, 2016.

Richter, J. H., Sassi, F., and Garcia, R. R.: Toward a Physically Based Gravity Wave Source Parameterization in a General Circulation Model, Journal of the Atmospheric Sciences, 67, 136–156, doi:10.1175/2009JAS3112.1, 2010.

Sato, K., Watanabe, S., Kawatani, Y., Tomikawa, Y., Miyazaki, K., and Takahashi, M.: On the origins of mesospheric gravity waves, Geophys. Res. Lett., 36, doi:10.1029/2009GL039908, 2009.

Stober, G., Sommer, S., Rapp, M., and Latteck, R.: Investigation of gravity waves using horizontally resolved radial velocity measurements, Atmos. Meas. Tech., 6, 2893–2905, doi:10.5194/amt-6-2893-2013, http://www.atmos-meas-tech.net/6/2893/2013/, 2013.

Xu, X., Wang, Y., Xue, M., and Zhu, K.: Impacts of Horizontal Propagation of Orographic Gravity Waves on the Wave Drag in the Stratosphere and Lower Mesosphere, J. Geophys. Res. Atmos., doi:10.1002/2017JD027528, http://dx.doi.org/10.1002/2017JD027528, 2017JD027528, 2017.

Interactive comment on Atmos. Chem. Phys. Discuss., https://doi.org/10.5194/acp-2017-644, 2017.

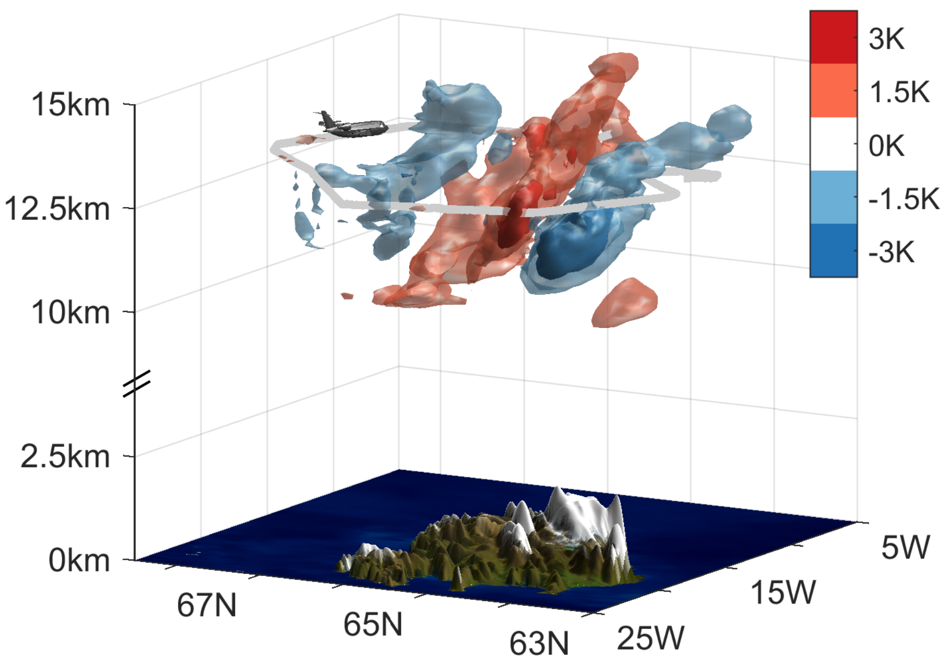

Fig. 1.

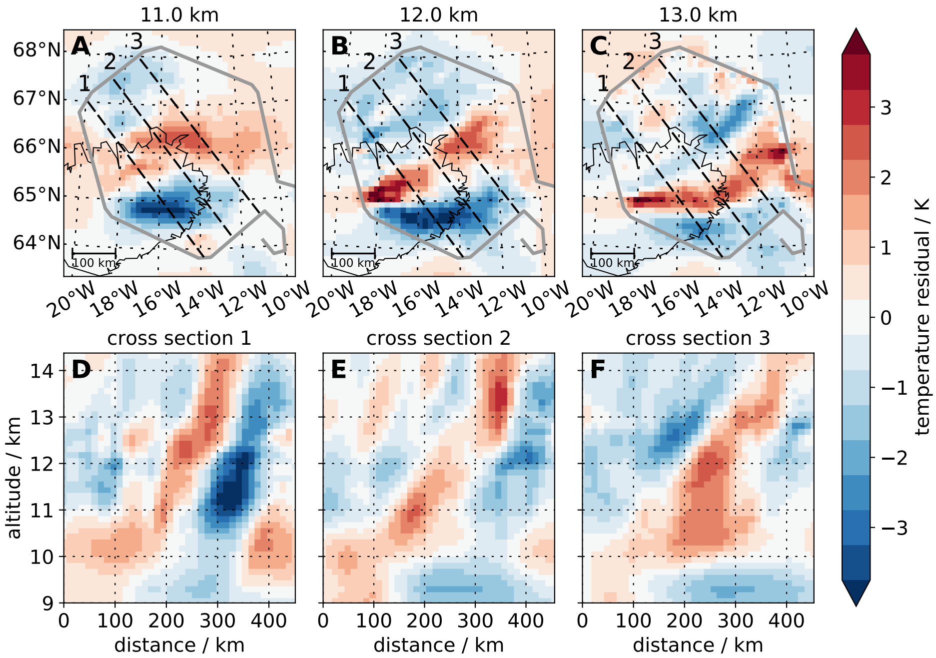
11.0 km
12.0 km
13.0 km
A
B
C
68°N
67°N
66°N
65°N
64°N
20°W 18°W 16°W 14°W 12°W 10°W
100 km
temperature residual / K
cross section 1
cross section 2
cross section 3
D
E
F
altitude / km
distance / km

Fig. 2.

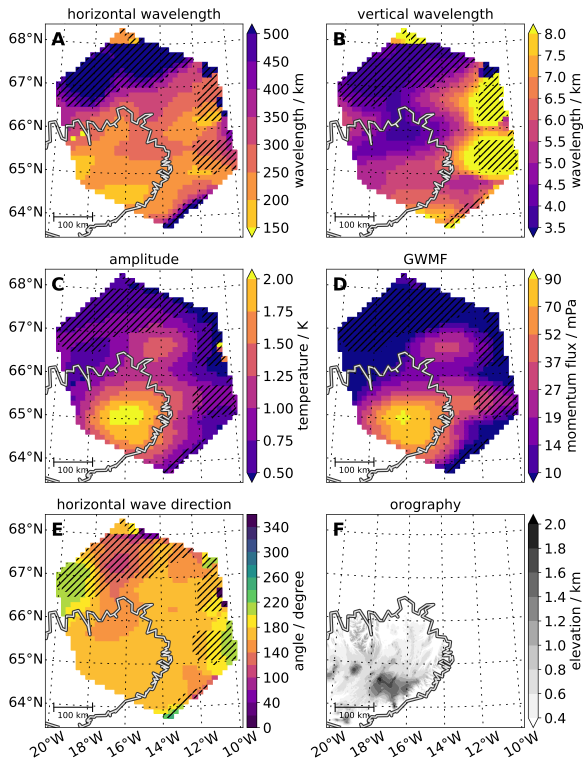
horizontal wavelength
vertical wavelength
amplitude
GWMF
horizontal wave direction
orography
wavelength / km
temperature / K
momentum flux / mPa
angle / degree
elevation / km
100 km
68°N
67°N
66°N
65°N
64°N
20°W 18°W 16°W 14°W 12°W 10°W

Fig. 3.